Published OnlineFirst February 5, 2015; DOI: 10.1158/1535-7163.MCT-14-0924

Molecular Cancer Therapeutics

Nonclinical Safety Evaluation of VX15/2503, a Humanized IgG4 Anti-SEMA4D Antibody

John E. Leonard, Terrence L. Fisher, Laurie A. Winter, Chad A. Cornelius, Christine Reilly, Ernest S. Smith, and Maurice Zauderer

Abstract

The humanized IgG4 monoclonal antibody VX15/2503 bound with 1 to 5 nmol/L affinity to purified recombinant semaphorin 4D (SEMA4D; CD100) produced using murine, rat, cynomolgus macaque, and human sequences. The affinity for native SEMA4D expressed on macaque T lymphocytes was approximately 0.6 nmol/L. Tissues from rats and cynomolgus macaques demonstrated specific staining only with resident lymphocytes. Single-dose and one-month toxicology/PK studies used VX15/2503 dose levels of 0 to 100 mg/kg. No toxicity was observed with either species in these studies, thus the no observed adverse effect level (NOAEL) was 100 mg/kg. C_{max}, exposure, and half-life values were similar for both rats and macaques. The NOAEL in a primate maximum feasible dose study was 200 mg/kg. Saturation of T-cell–associated SEMA4D occurred following administration of single doses of 0.1 mg/kg and above; five weekly injections of VX15/2503 at a dose level of 100 mg/kg produced saturation lasting for more than 120 and 130 days, respectively, for rats and primates. Macaques administered five weekly doses of VX15/2503 showed dose-dependent reductions of 2- to 3-fold in T-cell SEMA4D (cSEMA4D) expression levels compared with controls. Reduced cSEMA4D expression levels continued until serum antibody concentrations were 2 to 5 μg/mL, and thereafter normal cSEMA4D levels were restored. On the basis of these data, a phase I clinical study of the safety and tolerability of VX15/2503 was conducted, enrolling adult patients with advanced solid tumor diseases; a single-dose, dose escalation, phase I safety study was also initiated with subjects with multiple sclerosis. *Mol Cancer Ther; 14(4); 964–72. ©2015 AACR.*

Introduction

Semaphorins are a family of soluble and membrane-bound proteins originally characterized as axonal-guidance factors (1). These proteins play important roles in physiologic processes such as vascular growth, tumor progression, and immune cell regulation (2–4). Signaling cascades initiated by semaphorin 4D (SEMA4D) induce glial cell activation, neuronal process collapse, decreased oligodendrocyte precursor cell survival, migration and maturation, and disruption of endothelial tight junctions that preserve the integrity of the blood-brain barrier, all important processes in the initiation and progression of multiple sclerosis (5–8). Therefore, anti-SEMA4D antibodies may represent a new therapeutic strategy for not only cancer therapy, but also for the treatment of subjects with multiple sclerosis and other neuroinflammatory/neurodegenerative diseases as well.

SEMA4D is a 150-kDa transmembrane protein found predominantly on resting T lymphocytes and upregulated on other activated immune cells in the periphery. It contains a large N-terminal propeller "sema" domain followed by an Ig-like domain, a lysine-rich domain, a transmembrane domain, and a cytoplasmic tail with consensus tyrosine and serine phosphorylation sites. The molecule functions as both a receptor, signaling through its cytoplasmic domain, and as a ligand (4, 9). SEMA4D is expressed on the cell surface as a disulfide-linked homodimer (cSEMA4D) and upon cell activation, the extracellular domain can be released from the cell surface via proteolytic cleavage to generate a soluble, 240 kDa, homodimeric, physiologically active form of the protein (sSEMA4D; ref. 10).

SEMA4D is expressed abundantly on the surface of T lymphocytes and is weakly expressed on B lymphocytes, natural killer (NK) cells, monocytes, dendritic cells (DC), microglia, neurons, oligodendrocytes, and endothelial cells (11–13). Cellular activation stimulates upregulation of cSEMA4D on T cells, B cells, DCs, oligodendrocytes (14, 15), and platelets (16).

Three cellular receptors have been identified for SEMA4D: Plexin-B1 (PLXNB1), Plexin-B2 (PLXNB2), and CD72. PLXNB1, the high-affinity (1 nmol/L) SEMA4D receptor, is expressed in nonlymphoid tissues, including endothelial cells, some tumor cells, oligodendrocytes, and neurons (17). SEMA4D binding to PLXNB1 induces migration and activation of endothelial cells, and promotes migration of tumor cells (2, 4, 18). SEMA4D/PLXNB1 signaling also reportedly induces growth cone collapse of neurons, apoptosis of neural precursor cells, and process extension collapse and apoptosis of oligodendrocytes (19–23). PLXNB2 is an intermediate-affinity receptor for SEMA4D and binds predominantly to SEMA4C; it is reportedly expressed on keratinocytes and is thought to be involved in epidermal wound repair (24). CD72 binds SEMA4D with low affinity (K_D = 300 nmol/L) and is expressed on B cells, antigen-presenting cells, and platelets (12); it appears to act as a negative regulator of B-cell responses via the tyrosine phosphatase SHP-1 (25).

Vaccinex, Inc., Rochester, New York.

Note: Supplementary data for this article are available at Molecular Cancer Therapeutics Online (http://mct.aacrjournals.org/).

Corresponding Author: John E. Leonard, Vaccinex, Inc., 1895 Mount Hope Avenue, Rochester, NY 14620. Phone: 760-815-5969; Fax: 585-271-2765; E-mail: jleonard@vaccinex.com

doi: 10.1158/1535-7163.MCT-14-0924

Published OnlineFirst February 5, 2015; DOI: 10.1158/1535-7163.MCT-14-0924

IHC analysis of SEMA4D expression on tissues from several human tumor types showed that SEMA4D is overexpressed in urogenital, ovarian, pancreatic, head and neck, prostate, colon, breast, and lung cancers (ref. 26; E Smith, personal communication, 2008], and is produced by inflammatory cells and tumor-associated macrophages present in the tumor microenvironment (27, 28). Importantly, tumors coexpressing PLXNB1 and c-Met are characterized by worse clinical grading, increased incidence of lymph node metastases, and unfavorable clinical outcome (29).

Other studies suggest that SEMA4D may play multiple physiologic roles in the immune system (3, 12, 13, 30), including promotion of T-cell stimulation and B-cell aggregation and survival *in vitro* (31, 32). Also, the addition of SEMA4D-expressing cells or sSEMA4D enhances CD40-induced B-cell proliferation and immunoglobulin production *in vitro*, accelerates *in vivo* antibody responses (3, 25), and the presence of sSEMA4D inhibits immune cell migration; this effect is reversed by addition of anti-SEMA4D antibodies (10, 30).

Using a murine anti-SEMA4D antibody termed mAb 67-2, which bound to both murine and human SEMA4D, suppressed tumor growth of syngeneic and transgenic tumors (33), and moderated disease symptoms in neurodegenerative disease models of multiple sclerosis (15). Vaccinex scientists created VX15/2503, a humanized IgG4 antibody with high affinity for rodent, nonhuman primate, and human SEMA4D (15, 33). The nonclinical safety studies described in this work characterized the pharmacokinetics, toxicology, and pharmacodynamics of VX15/2503 in rats and cynomolgus macaques. Collectively, these data supported the evaluation of VX15/2503, a humanized, high-affinity IgG4 monoclonal anti-SEMA4D antibody, as an investigational agent in trials enrolling adult patients with advanced solid tumors, and in the treatment of subjects with multiple sclerosis.

Materials and Methods

Production cell line and antibodies

VX15/2503 is a humanized IgG4 mAb generated from the murine antibody 67-2 (33). A hinge mutation was introduced to prevent *in vivo* Fab arm recombination (34); the characterization of VX15/2503 is described elsewhere (15, 33, 35, unpublished observations). VX15/2503 was expressed by a proprietary CHO cell line constructed by Catalent Pharma Solutions; the sequences of the retrovector protein coding regions were verified by analysis. The expression construct was selected based on growth and viability characteristics, antibody expression titer and clonal stability; production cells were tested according to Good Manufacturing Practice guidelines. The expressed antibody was purified using standard techniques, formulated at 20 mg/mL in sodium acetate buffer, pH 5.4, and tested for functional potency, etc., before release. Formulated VX15/2503 was stable for >36 months at 5 ± 3°C.

A second humanized IgG4 anti-SEMA4D antibody, mAb 2282, binds to an epitope distinct from that recognized by VX15/2503 (ref. 35; unpublished observations) and was used as a reagent in assays with primate sera as it recognizes only primate and human SEMA4D.

In vitro studies

Affinity determinations using surface plasmon resonance (SPR) kinetic analysis were performed using a Biacore 2000 system. Recombinant 6× histidine-tagged SEMA4D was expressed as a stable transfectant in CHO cells and purified from culture supernatants using a standard Ni column. Supplementary Methods provide additional details.

GLP tissue cross reactivity studies were performed using fresh-frozen rat and primate tissues incubated with biotinylated VX15/2503. The biotin-antibody conjugation ratio was ≤2:1 and biotinylation had no effect on binding to SEMA4D. VX15/2503 was used at concentrations of 0.625 to 2.5 μg/mL. Thirteen rat and 14 macaque tissues from three donors, as well as positive and negative control tissues, were evaluated using biotinylated VX15/2503 or a biotinylated isotype control. Tissues were assessed for suitability before each experiment. 3,3'-diaminobenzidine (DAB) substrate chromogen was used to identify bound antibody and stained tissues were evaluated by peer review.

A flow cytometry–based method similar to that used by Heider (36) was used to measure the affinity of VX15/2503 for primate T-cell cSEMA4D. Isolated peripheral blood mononuclear cells (PBMC) from five different macaques were incubated with various concentrations of VX15/2503 for 1 hour at 4°C, washed, and then incubated with a monoclonal FITC–anti-human IgG4 Fc secondary antibody for 30 minutes at 4°C. Quantum FITC molecules of equivalent soluble fluorochrome (MESF) beads (Bang's Labs) were utilized to generate a standard curve to convert geometric mean fluorescence intensity (GMFI) to MESF. A modified Scatchard analysis was used to calculate the binding affinity (K_D) of VX15/2503 to cSEMA4D.

In vivo studies

All procedures were conducted in compliance with the Animal Welfare Act, the Guide for the Care and Use of Laboratory Animals, and the Office of Laboratory Animal Welfare. All protocols were approved by appropriate Institutional Animal Care and Use Committees; both rat and all three cynomolgus macaque studies were GLP and ICH compliant.

Single and repeat doses of VX15/2503 were administered to both rats and cynomolgus macaques using standard procedures. Single-dose studies were performed using dose cohorts of 0, 0.01, 0.1, 1.0, 10, and 100 mg/kg to determine toxicity, PK, pharmacodynamics (PD), and immunogenicity of VX15/2503. Antibody was administered in the tail vein (rats) or saphenous vein (cynomolgus macaques). Test article or control was delivered over 5 minutes (rats) or 15 minutes (macaques); animals were observed for 4 hours following infusion. Weekly immunophenotypic evaluation of lymphocyte subsets was performed using blood from both species; ECG and standard clinical observations were also performed at these time points. No rat necropsies were performed in the single-dose study but necropsies were performed on each primate to evaluate changes in gross pathology; a standard panel of tissues was collected for analysis. The repeat-dose studies evaluated five weekly i.v. doses of VX15/2503 at dose levels of 0, 10, 30, or 100 mg/kg; similar observations and study endpoints were included in studies of both species as in the single-dose studies. See Supplementary Methods for additional details.

A subsequent GLP single-dose primate (MFD) study evaluated dose levels of 100 and 200 mg/kg; 5 animals per sex were used in the control and each dose cohort. A maximum volume of 10 mL/kg was administered to each animal; blood samples were analyzed for cSEMA4D saturation levels. Three animals per sex per group were sacrificed 14 days after dosing and the tissues analyzed by histopathology.

Published OnlineFirst February 5, 2015; DOI: 10.1158/1535-7163.MCT-14-0924

A rat host resistance study (37, 38) was conducted using animals dosed weekly for 8 weeks with VX15/2503 and inoculated via nasal aspiration with a rat-adapted flu virus at week 5 (15); antibody dose levels used were 10, 100, and 200 mg/kg. Control groups consisted of naïve animals, vehicle-treated animals, and animals dosed daily with 2 mg/kg of dexamethasone. Animals were sacrificed at week 9. Study assessments included determination of influenza titer using lung tissue homogenates on postinfection study days 1, 2, 8, and 21, influenza-specific IgG and IgM responses on days 1, 2, 8, and 21, NK cell activity (by chromium release) on study day 2, T-cell activity on day 8, and periodic clinical signs and body weight determinations (15, 38). Blood samples were analyzed to quantitate various lymphocyte subsets.

Standard immunophenotypic analyses were used in the various studies described above to assess lymphocyte subset levels before and following VX15/2503 administration. Animal blood samples were evaluated using Multitest TBNK reagents (BD) and samples were analyzed on a BD FACS Canto II.

Detection of VX15/2503 in serum was performed using a validated ELISA. The assay utilized recombinant marmoset SEMA4D (Vaccinex) as a capture reagent and a mouse anti-human IgG4 antibody labeled with horseradish peroxidase (HRP; Southern Biotech); TMB (3,3′,5,5′-tetramethylbenzidine) was used as the detection reagent. The lower limit of quantitation of this assay was 1.0 ng/mL, whereas the upper limit was 30 ng/mL; the minimum required dilution was 1:5. Specimens were stabile for a minimum of 6 months at −60 to −80°C.

Pharmacokinetic assessments of VX15/2503 in sera from the single- and repeat-dose macaque studies and from the one-month rat study were performed by noncompartmental analysis using WinNonlin version 5.2 (Pharsight Corporation). See Supplementary Methods section for additional details.

Detection of anti-VX15/2503 (ADA) responses generated in toxicology studies used a modified affinity capture elution (ACE) ELISA previously described (39). Microtiter plates were coated with VX15/2503 to capture ADA complexes and acid-released ADA was used to coat fresh plates. Biotinylated VX15/2503 was used to detect captured anti-VX15/2503 antibodies. Animal serum samples were stable for a minimum of 3 months when stored at −60 to −80°C.

A flow-cytometric assay was performed to assess VX15/2503 saturation of cSEMA4D on primate T lymphocytes. Whole blood was lysed and cells were incubated with an isotype control, an anti-human IgG4, or anti-human IgG4 plus excess VX15/2503. The percentage of T-cell saturation was determined by measuring differences in GMFI values of T cells previously incubated with anti-human IgG4 versus the maximum saturation as determined by addition of anti-human IgG4 plus excess VX15/2503.

The humanized anti-SEMA4D antibody mAb 2282 was used to determine changes in cellular expression of primate cSEMA4D in response to VX15/2503. Differences in cSEMA4D expression were determined cytofluorometrically based on the shift in mean fluorescence intensity determined using T lymphocytes from treated animals versus T cells from control animals. Cellular SEMA4D saturation values of 20% and below were considered to be unsaturated.

Two qualified ELISAs were utilized to measure total sSEMA4D levels. Baseline sSEMA4D levels in rats were determined using a mouse monoclonal anti-rodent SEMA4D antibody. Diluted serum samples were added to coated plates and a biotinylated, noncompeting murine anti-SEMA4D antibody was added. Plates were analyzed using standard techniques. Concentrations of sSEMA4D were calculated by comparing absorbance at $A_{450-650\ nm}$ to that of a recombinant rat sSEMA4D reference standard. This assay was linear for sSEMA4D concentrations from 31 to 2,000 pg/mL.

A second system was used for evaluation of total sSEMA4D in primate sera at baseline and following VX15/2503 administration. This ELISA utilized mAb 2282 to capture the sSEMA4D, whether free or complexed with VX15/2503. Complexed and free sSEMA4D was detected using a noncompeting biotinylated secondary reagent followed by addition of streptavidin-HRP and TMB substrate. Serum concentrations of total sSEMA4D were calculated as described above, using recombinant cynomolgus macaque sSEMA4D as a reference standard. This assay was linear over the concentration range of 37 to 500 pg/mL.

Results

VX15/2503 characterization

VX15/2503 bound with approximately 3 to 5 nmol/L affinity to rodent, primate, and human recombinant sSEMA4D by SPR analysis; similar results were obtained with mAb 67-2. Interestingly, analysis of VX15/2503-binding data derived using macaque T lymphocytes demonstrated that the affinity of VX15/2503 for native macaque cSEMA4D was approximately 0.6 nmol/L (Fig. 1).

GLP tissue cross-reactivity studies with VX15/2503 showed that the antibody bound to infiltrating lymphocytes in tissues from both rats and primates (not shown). Rat lymphocyte reactivity was observed only with spleen sections, while macaque tissues showed specific reactivity with residential or infiltrating lymphocytes in blood, ileum, colon, spleen, and tonsil. The cellular membranes of glandular epithelial cells in primate uterine endometrium were also reactive. Nonspecific reactivity was not observed.

Mean pharmacokinetic parameters determined for VX15/2503 in sera collected in rat and macaque single-dose studies are shown in Table 1. The half-life for rats in the 10 mg/kg dose cohort

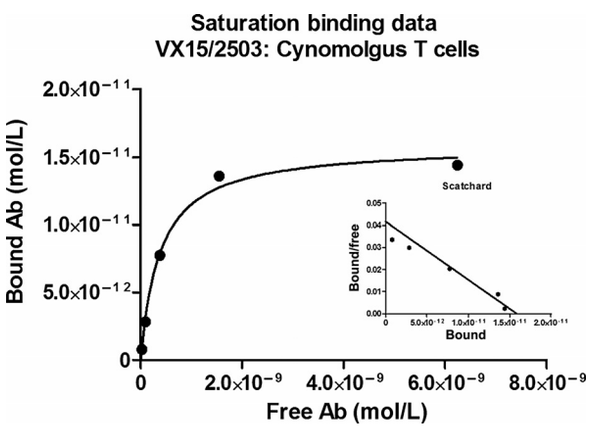

Figure 1.
Binding of VX15/2503 to native SEMA4D expressed on cynomolgus macaque peripheral blood T lymphocytes. Peripheral blood mononuclear cells from five different cynomolgus macaques were assayed; shown are the mean values of the results obtained for VX15/2503 binding to $CD3^+$ T lymphocytes from these samples. The Scatchard analysis was performed using a method similar to that described by Heider et al. (36); the determined K_D was 0.6 nmol/L.

Published OnlineFirst February 5, 2015; DOI: 10.1158/1535-7163.MCT-14-0924

Table 1. Mean pharmacokinetic values determined for rats and cynomolgus macaques following single intravenous administration of VX15/2503

	Rat[a]				Cynomolgus macaque[b]			
Dose	C_{max}	AUC_{0-t}	Half-life		C_{max}	AUC_{0-t}	Half-life	
(mg/kg)	(μg/mL)	(μg/h/mL)	(d)	(h)	(μg/mL)	(μg/h/mL)	(d)	(h)
0.01	NC[c]	NC	NC	NC	0.075	0.312	NC	NC[c]
0.1	1.99	11.40	0.1	3.5	2.98	23.21	NC	NC
1.0	34.14	834.7	1.2	27.8	40.8	1,898	NC	NC
10	317.7	27,431	4.4	105.7	342	37,423	NC	NC
100	3,305	488,194	10.3	246.2	3,785	725,672	9.0	215

NOTE: Rat PK data were derived from a single compartment two-phase pharmacokinetic modeling with male and female data combined. Antibody was administered intravenously over a period of roughly 5 minutes; 3 animals of each gender were in each dose group. Similar results were obtained following separate analyses of data from males and from females. Primate PK data were derived from a noncompartmental analysis with 2 animals of each gender in each dose group. Data shown are for males and females combined; similar results were obtained following separate analyses of data from males and females.

[a]Based on single compartment two-phase pharmacokinetic modeling. Three animals of each gender were included in each dose group.

[b]Based on noncompartmental analysis with 2 animals of each gender in each dose group.

[c]Insufficient data to perform the calculation.

approximated that obtained for a single similar dose of mAb 67-2 administered to mice (not shown). Nonlinear pharmacokinetics were noted for both species when comparing increases in exposure values as a function of dose levels. Figure 2 illustrates mean VX15/2503 serum concentrations as a function of time for rats and primates following single antibody doses.

Mean PK values determined for male and female rats and macaques in the one-month toxicology studies were similar for both species. The half-life of VX15/2503 following the fifth dose at 100 mg/kg was roughly 12 days for both rats and primates. C_{max} increases were roughly dose proportional, with respective values for rats and macaques in the 10 mg/kg dose cohorts being 226 and 292 μg/mL; combined values for males and females in the 100 mg/kg dose cohorts were 7,115 and 7,697 μg/mL for rats and primates, respectively. Exposure values for rats ranged from 23,653 to 1,345,350 μg/h/mL for animals in the 10, 30, and 100 mg/kg cohorts, respectively; primate values were similar. VX15/2503 exposure in the macaque MFD study increased roughly proportionally with dose level; respective AUC values for the 100 and 200 mg/kg dose cohorts were 605,254 and 1,430,122 μg/h/mL.

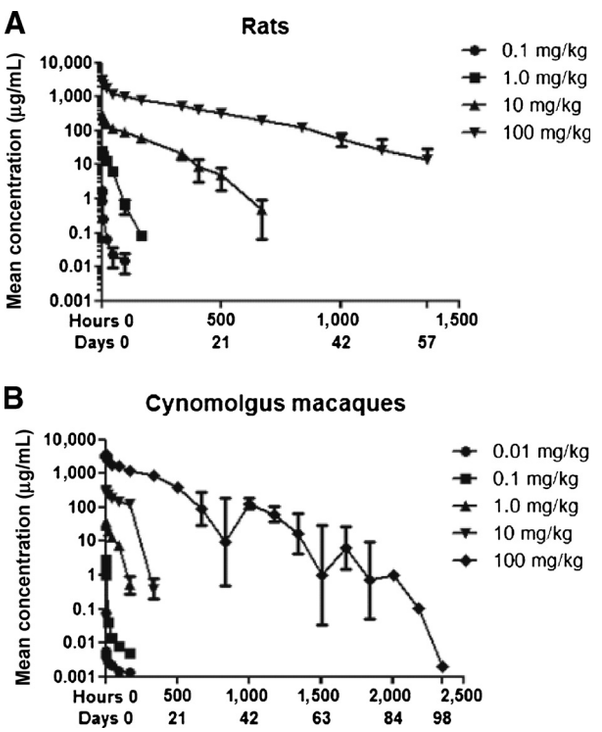

Figure 2.
Serum VX15/2503 concentration versus time plots for rats and cynomolgus macaques following a single intravenous administration of VX15/2503. Three animals of each gender were assigned to each dose group for the rat single-dose study (A); the macaque study used 4 males and 4 females in the control group and 2 animals of each gender in each dose cohort (B). The data shown for each dose level are for males and females combined; error bars, ± SD.

Toxicology assessments

Both rats and primates tolerated single i.v. VX15/2503 doses in the range of 0.01 to 100 mg/kg. The body weights of study animals increased during these studies and no adverse effects were apparent in the clinical and anatomic pathology parameters evaluated. Sporadic changes that occurred in food consumption and fecal consistency were transient and considered typical for institutional macaque colonies (40). Rats were observed predose, on the day of dose administration, and for up to 57 days postdose, as determined empirically by T-cell cSEMA4D desaturation. All rats survived to the scheduled sacrifice date except for one high-dose male that became moribund following blood collection on day 57. Cynomolgus macaques in the single-dose study were observed for up to 120 days after dosing, as determined by the kinetics of cSEMA4D desaturation. Toxicology results for macaques treated at the 100 and 200 mg/kg dose levels in the MFD study were similar to those described above for macaques in the single-dose study.

Rats were administered five weekly doses of VX15/2503 in the one-month toxicology study. All rats tolerated dose administration and all animals survived to their scheduled sacrifice dates with the exception of two that died as a result of blood collection errors. Mean body weights of study animals increased during the course of the study and clinical chemistry and hematology values were unaffected by VX15/2503 administration. No clinically relevant changes were noted in physical examinations.

As reported elsewhere (15), no adverse test-article effects were noted in assessments made during the rat host resistance study. However, rats in the dexamethasone-treatment cohort exhibited body weight reductions of 44% and 17% for males and females, respectively. These body weight decreases occurred after 4 days of

Published OnlineFirst February 5, 2015; DOI: 10.1158/1535-7163.MCT-14-0924

dosing and were consistent with published effects of steroid treatment (37, 38). Spleen and lung organ weights were similarly reduced.

The one-month cynomolgus macaque study was performed using the same dosing regimen as that used in the rat study. Five weekly i.v. doses of VX15/2503 were well tolerated and all animals survived until their scheduled sacrifice dates. No toxicologically important changes were noted in body weights or in various other physical examination parameters. Blood chemistry and hematology parameter changes were clinically insignificant.

No changes were observed in T cell (total, helper, cytotoxic), B cell, NK cell, or monocyte levels in primates in the single dose or MFD toxicology studies, or in the one-month repeat-dose studies involving rats and primates. Lymphocyte levels were not evaluated in the single-dose rat study.

However, compared with baseline values, a statistically significant decline of 40% to 60% was observed in absolute and percent NK cell levels for rats in all VX15/2503 treatment groups in the one month study; no changes were noted in T cell (total, helper, cytotoxic), B cell, or monocyte levels. No correlation was observed between dose level and the extent of NK cell reduction. By the end of the recovery period, NK values for control male and female rats had also decreased to levels for treated animals. The reduction of NK cells in treated animals was not correlated with any change in clinical or anatomic observations. No comparable reductions in NK cell levels were observed in the macaque repeat-dose study.

Similar lymphocyte and NK cell findings were observed in male and female rats by day 8 postinfection in the host resistance model study (Fig. 3). Although no changes were observed in B- and T-lymphocyte levels in blood or splenic tissue from antibody-treated animals, statistically significant reductions of 33% to 56% in NK cell levels (compared with controls) were observed in antibody-treated males and females at the doses used. Steroid-treated animals showed similar reductions in NK cell levels compared with controls. Only slight changes were noted in $CD4^+$ T lymphocyte and in cytotoxic T-cell levels in peripheral blood and in splenic samples collected postinfection on study days 2 and 8 for all antibody dose groups (not shown).

Influenza viral infection in the rat host resistance study occurred at week 5 of the 8-week VX15/2503 dosing sequence. Viral titers peaked in all animals 24 hours postinoculation and decreased sharply thereafter for all VX15/2503 treatment groups, reaching baseline on day 8 postexposure (15). Rats treated with dexamethasone, however, exhibited delayed viral clearance, reaching baseline 21 days postinfection.

VX15/2503 treatment in the host resistance study affected, by day 2, a roughly 40% reduction in NK cell activity in lung samples from animals in the 10 and 100 mg/kg dose groups (Fig. 4); splenic effects were similar (not shown). No similar effect was seen in animals treated at 200 mg/kg. Steroid-treated animals showed a 58% reduction in NK activity but no effects were observed on cytotoxic T-cell activity levels in lung tissue from antibody-treated animals (not shown). However, dexamethasone treatment reduced CTL activity to undetectable levels in those animals.

T-dependent antibody responses showed a statistically significant decrease of 33% in the influenza-specific IgM response (day 8 postinfection) for animals treated with VX15/2503 (not shown); on day 21, these animals exhibited a 26% reduction in the influenza-specific IgG response. Viral clearance was unaffected in antibody-treated animals (15). Steroid-treated rats also exhibited typically reduced viral-specific IgM and IgG responses (37, 38); compared with vehicle-treated controls, the IgM response (day 8) was reduced by 70%, whereas the IgG response (day 21) was reduced by 92%.

T-cell cSEMA4D saturation was observed for all macaques administered a single VX15/2503 dose of 0.1 mg/kg or higher (Fig. 5A). Data suggest that the serum antibody concentration required to achieve complete cSEMA4D saturation was 2 to 5 μg/mL. One hour after VX15/2503 infusion at 0.1 mg/kg, macaque cSEMA4D was completely saturated; by day 2, however, saturation was undetectable. Maximal cSEMA4D saturation was noted through day 7 for animals administered single doses of 1.0 or 10 mg/kg, and through at least day 49 for macaques administered, a single dose of 100 mg/kg. Similar results were obtained for rats administered single doses of 10 or 100 mg/kg VX15/2503, producing cSEMA4D saturation through days 14 and 42, respectively.

Prolonged, dose-dependent cSEMA4D saturation was noted for rats and primates treated in the one-month studies. Maximal cSEMA4D saturation was sustained through days 29 and 141, respectively, for macaques in the 10 or 100 mg/kg dose cohorts (Fig. 5B). Macaques in the 30 mg/kg dose cohort were not evaluated. Rats administered repeat doses of VX15/2503 exhibited maximal cSEMA4D saturation through days 29, 78, and 120, respectively, for animals treated at 10, 30, or 100 mg/kg (not shown).

In vitro studies using primary cultures of human and primate T cells demonstrated that the VX15/2503-cSEMA4D complex on T cells was rapidly internalized following antibody binding, with roughly 60% of the complex internalized after 24 hours at 37°C (ref. 35; unpublished observations). Administration of five weekly doses of VX15/2503 to cynomolgus macaques resulted in dose-dependent reductions in cSEMA4D levels for animals in all dose groups. T lymphocytes from high-dose animals after the fifth dose expressed on average 2- to 3-fold less cSEMA4D than control animals, and reduced cSEMA4D expression continued throughout the recovery period until serum antibody levels dropped below 2 to 5 μg/mL (day 190). Cellular SEMA4D levels for mid-dose macaques were not evaluated. No similar studies were performed with rat T cells because mAb 2282 recognizes only primate and human SEMA4D.

Baseline sSEMA4D levels were determined for naïve rats and macaques. The mean value determined from 23 rat samples was 24.5±1.9 ng/mL (range 8 to 46 ng/mL); the similar baseline value for 20 cynomolgus macaques was 117.7±11.3 ng/mL (range 39 to 234 ng/mL). Following administration of repeat doses of VX15/2503, sSEMA4D levels increased approximately 39-fold for primates administered 100 mg/kg and remained elevated during the course of VX15/2503 administration; sSEMA4D levels declined following cessation of dosing, returning to baseline levels by the end of the recovery period (not shown). No similar results were obtained with rat sera because the MAb2282-based assay cannot detect the VX15/2503–sSEMA4D complex.

Antibodies to VX15/2503 (ADA) were detected in the sera of most animals in the single-and repeat-dose studies; these responses were typically observed within the first 2 weeks of dosing. Although 4 of 6 rats treated with a single dose of VX15/2503 at 0.01 mg/kg produced an immune response, 20 of 26 animals treated at 0.1, 1, or 10 mg/kg developed anti-VX15/2503 antibodies. Immune response titers were

Published OnlineFirst February 5, 2015; DOI: 10.1158/1535-7163.MCT-14-0924

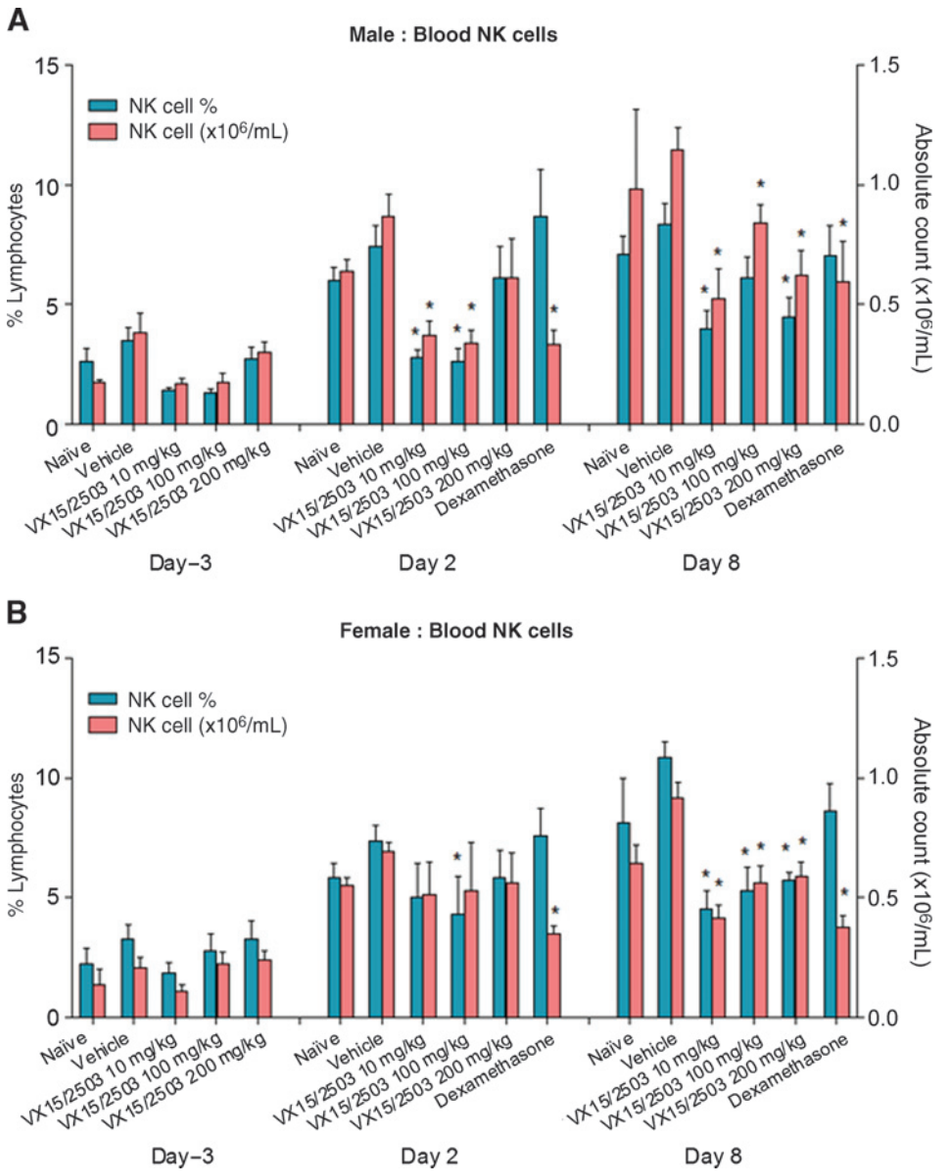

Figure 3.
NK cell levels in blood of rats treated with VX15/2503 or dexamethasone. Animals were treated with vehicle, VX15/2503 (at the dose levels shown) or dexamethasone as described in the Materials and Methods section. The ordinate label (percentage of lymphocytes) refers to the percentage of $CD3^{-}$, $CD161a^{+}$ NK cells (represented by blue bars) in the blood of males (A) or females (B). *, $P < 0.05$, difference from vehicle control results.

highest in animals treated with single VX15/2503 doses of 0.01, 0.1, or 1 mg/kg; ADA responses became evident by day 15 and peaked between study days 35 and 42. No immune response was observed for rats treated with single VX15/2503 doses of 10 or 100 mg/kg until VX15/2503 began to be cleared from the serum, between days 14 and 42. Similar results were seen in the single-dose primate study, with 2 of 4 animals administered 0.01 mg/kg of VX15/2503 producing an immune response, and all 42 macaques treated with single or repeat doses of 0.1, 1, 10, 30, or 100 mg/kg exhibiting ADA (not shown).

Rats administered repeat doses of 10, 30, or 100 mg/kg of VX15/2503 exhibited immune responses in 100%, 78%, and 44% of the animals, respectively. Rats in the one-month study treated with a dose of 100 mg/kg exhibited a low response until cessation of dosing, which then increased during the recovery phase (not shown). Results for treated macaques were similar, with 2 of 4 animals administered a single dose of 0.01 mg/kg producing an immune response; all 42 macaques treated with single or repeat doses of 0.1, 1, 10, 30, or 100 mg/kg exhibiting anti-VX15/2503 antibodies.

Discussion

We have characterized the pharmacokinetic, pharmacodynamic, and toxicologic properties of the humanized anti-SEMA4D antibody VX15/2503 in both single- and repeat-dose studies using rats and primates. The affinity of the antibody for macaque, native cellular SEMA4D was roughly 10-fold lower than that determined using recombinant SEMA4D using the SPR assay, perhaps due to conformational changes that occurred during the expression and/or attachment of the recombinant protein to the Biacore assay surface. Tissue reactivity profiles obtained with VX15/2503-

Published OnlineFirst February 5, 2015; DOI: 10.1158/1535-7163.MCT-14-0924

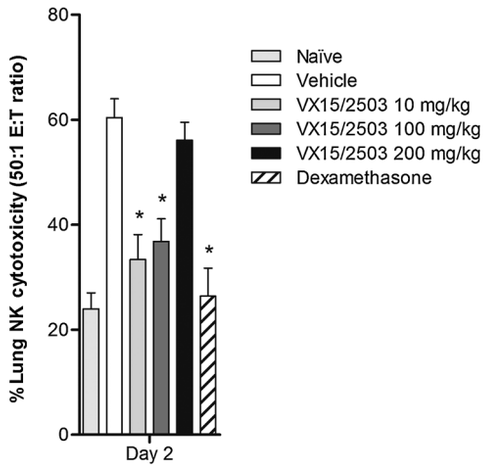

Figure 4.
NK cell activity in lung samples of virally infected rats as percent cytotoxicity. NK cell function was assessed using lung homogenates prepared on day 2 post viral infection and YAC-1 target cells prelabeled with chromium-51 as described (39). Values represent group mean values ± SE for males and females combined. Data shown are for an effector-target ratio of 1:50.
*, $P < 0.05$, difference from vehicle control results.

treated rat and macaque specimens showed a restricted pattern of reactivity. Thus, these *in vitro* data suggest that rats and primates were appropriate for use in the pharmacologic and toxicologic assessment of VX15/2503.

As suggested by the tissue reactivity studies, evaluation of VX15/2503 in GLP single- or repeat-dose toxicology studies using rats or primates produced no clinical or anatomic findings of any significance. The no observed adverse effect level (NOAEL) was the highest dose tested, 100 mg/kg for rats and primates in the single-dose and one-month studies, and 200 mg/kg for primates in the MFD study. Finally, the rat host resistance study showed that VX15/2503 was non-immunosuppressive (15).

The pharmacokinetic behavior of i.v. administered VX15/2503 was similar in both rats and macaques. The C_{max} and $AUC_{0\text{-}t}$ values were similar in the single- and repeat-dose studies of both species, and the antibody clearance profiles were also similar over the dose range evaluated (Fig. 2). Exposure was generally dose dependent and increased with dose and dose frequency in both sets of studies.

As suggested by the antibody clearance profiles (Fig. 2), nonlinear pharmacokinetics of VX15/2503 were observed in primates immediately after dosing and when serum antibody concentrations were <5 μg/mL. At low-serum antibody concentrations, the apparent rapid clearance of VX15/2503 from serum of treated animals was likely due to VX15/2503 binding to both soluble and cellular SEMA4D. In addition, our data suggest that the cellular antibody–receptor complex is internalized. The rapid clearance of low concentrations of VX15/2503 from the periphery may be due to target-mediated disposition (41), accounting for the precipitous drop in serum VX15/2503 concentrations apparent in the 10 and 100 mg/kg dose cohorts in the single-dose primate study. Similar rapid serum clearance has been described for an anti-αv integrin monoclonal antibody (42).

The reduction in levels of NK cells noted in the repeat-dose rat study was surprising given the absence of Fc receptor binding or cytolytic activity by VX15/2503 (43). No similar finding was observed in the repeat-dose primate study. As reductions in both NK activity and cellular levels were also observed in the host resistance study, these NK cell effects may be due to a pharmacologic property of VX15/2503 at dose levels of 100 mg/kg and below. As these findings were not correlated with any change in clinical parameters, they were not considered adverse. Why this same effect was not observed at the 200 mg/kg dose level is unknown.

Immunogenicity is commonly observed in animals administered a humanized antibody (44). Anti-VX15/2503 responses were produced in most treated animals from either species, regardless of whether the animals received single or repeated doses. Animals administered 10 mg/kg VX15/2503 or less exhibited higher anti-VX15/2503 antibody titers than animals dosed at 30 or 100 mg/kg. Thus, anti-VX15/2503 antibodies exerted a larger impact on VX15/2503 exposure at lower dose levels. Conversely, anti-VX15/2503 responses in animals treated at the mid- and high-dose levels were much lower than in the low-dose treatment groups. Sufficiently high concentrations of VX15/2503 were found in the sera of most single and repeat-dose animals in the mid- and high-dose groups to allow for exposure to high-serum concentrations of VX15/2503, and thus the evaluation of toxicities that may have arisen from VX15/2503 administration.

The ACE-ELISA technique used in this work is typically able to detect anti-drug antibody in the presence of a 1,000-fold excess drug (39). In the single-dose rat study, anti-VX15/2503 antibody responses were undetectable when the average VX15/2503 serum concentration was >200 μg/mL. Once below this threshold moderate immunogenicity was detectable, suggesting that the

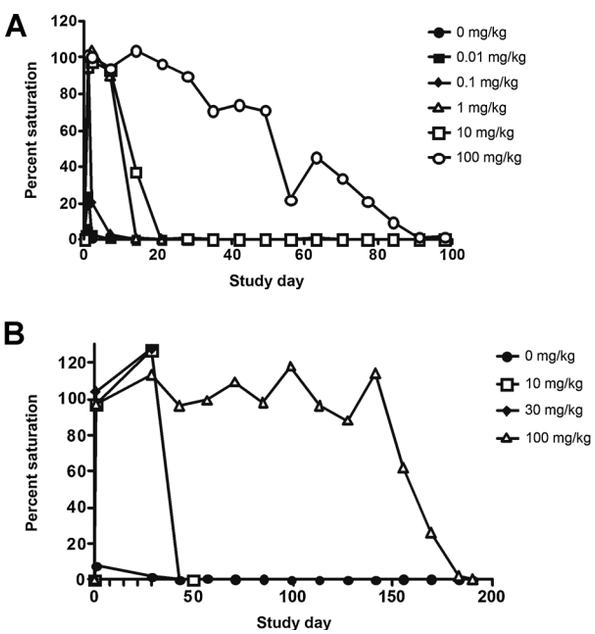

Figure 5.
T-cell–associated SEMA4D saturation versus time profiles for cynomolgus macaques administered either single or five weekly i.v. doses of VX15/2503. Two to 7 animals of each gender were assigned to each dose group for the single-dose study (A) and repeat-dose study (B); exact numbers are provided in the Materials and Methods section. Data shown for each dose level are for males and females combined. Similar results were obtained following separate analysis of data from males or from females (not shown).

circulating antibody masked detectable immunogenicity when the antibody was in excess of 1,000-fold. Thus our results may underestimate the amount of anti-VX15/2503 antibodies present in the serum of animals treated with high doses of VX15/2503.

VX15/2503 administration to rats and cynomolgus macaques at most dose levels produced prolonged saturation of cSEMA4D. Moreover, the resulting saturation profiles closely mirrored the serum antibody concentration profiles (Figs. 2B and 5A), suggesting that the serum VX15/2503 concentration required to achieve complete cSEMA4D saturation in cynomolgus macaques was approximately 2 to 5 μg/mL.

Disappearance of cSEMA4D from the T-cell surface was apparent after VX15/2503 administration, and was reversible following cessation of antibody treatment. Similar results were reported for the CD20 antigen following addition of an anti-CD20 antibody (45). As observed with the CD20 antigen–antibody complexes, cSEMA4D expressed on primate PBMCs cultured *in vitro* was internalized following VX15/2503 binding (ref. 35; unpublished observations). The fate of the internalized VX15/2503–cSEMA4D complex remains to be elucidated.

Gordon and colleagues (46) showed that levels of the secreted antigen VEGF increased substantially following bevacizumab administration. Similarly, sSEMA4D levels increased following single and repeated VX15/2503 administration to cynomolgus macaques, likely due to a reduction in sSEMA4D clearance following formation of the antigen–antibody complex.

The safety studies of VX15/2503 described above demonstrated that the antibody was well tolerated and produced no clinical or toxicologic findings of consequence. These data supported the use of VX15/2503 in a safety and tolerability phase I clinical study in patients with advanced solid tumors (NCT01313065; now completed). In addition, when taken together with data from the macaque MFD study, these data supported the evaluation of VX15/2503 in a single ascending dose, safety and tolerability study in multiple sclerosis subjects (NCT01764737; enrollment and treatment completed). Future trials will use the combination of VX15/2503 with immunomodulatory agents in the treatment of advanced solid tumor patients.

Disclosure of Potential Conflicts of Interest

J.E. Leonard has ownership interest (including patents) in Vaccinex, Inc. T.L. Fisher has ownership interest in patents and stock options in Vaccinex, Inc.. M. Zauderer has ownership interest in the Vaccinex, Inc. No potential conflicts of interest were disclosed by the other authors.

Authors' Contributions

Conception and design: J.E. Leonard, T.L. Fisher, C.A. Cornelius, E.S. Smith, M. Zauderer

Development of methodology: T.L. Fisher, L.A. Winter, C.A. Cornelius, E.S. Smith

Acquisition of data (provided animals, acquired and managed patients, provided facilities, etc.): J.E. Leonard, L.A. Winter

Analysis and interpretation of data (e.g., statistical analysis, biostatistics, computational analysis): J.E. Leonard, T.L. Fisher, L.A. Winter, C.A. Cornelius, M. Zauderer

Writing, review, and/or revision of the manuscript: J.E. Leonard, T.L. Fisher, L.A. Winter, C.A. Cornelius, C. Reilly

Administrative, technical, or material support (i.e., reporting or organizing data, constructing databases): J.E. Leonard, T.L. Fisher, L.A. Winter, C.A. Cornelius, C. Reilly

Study supervision: J.E. Leonard, T.L. Fisher, C.A. Cornelius, M. Zauderer

Acknowledgments

The authors thank Jennifer Seils for technical assistance, Donna Meleca for administrative support in the preparation of this article, and Covance Laboratories, Inc., for study management.

Grant Support

This work was funded solely by company resources.

The costs of publication of this article were defrayed in part by the payment of page charges. This article must therefore be hereby marked *advertisement* in accordance with 18 U.S.C. Section 1734 solely to indicate this fact.

Received October 21, 2014; revised January 12, 2015; accepted January 29, 2015; published OnlineFirst February 5, 2015.

References

1. Barton W, Himanen J, Antipenko A, Nikolov D. Structures of axon guidance molecules and their neuronal receptors. Adv Protein Chem 2004;68: 65–106.
2. Conrotto P, Corso S, Gamberini S, Comoglio PM, Giordano S. Interplay between scatter factor receptors and B plexins controls invasive growth. Oncogene 2004;23:5131–7.
3. Ishida I, Kumanogoh A, Suzuki K, Akahani S, Noda K, Kikutani H. Involvement of CD100, a lymphocyte semaphorin, in the activation of the human immune system via CD72: implications for the regulation of immune and inflammatory responses. Int Immunol 2003;15: 1027–34.
4. Basile JR, Barac A, Zhu T, Guan KL, Gutkind JS. Class IV semaphorins promote angiogenesis by stimulating Rho-initiated pathways through plexin-B. Cancer Res 2004;64:5212–24.
5. Prineas J. Pathology of the early lesion in multiple sclerosis. Hum Pathol 1975;6:531–54.
6. Adams CW. Pathology of multiple sclerosis: progression of the lesion. Br Med Bull 1977;33:15–20.
7. Pierson E, Simmons SB, Castelli L, Goverman JM. Mechanisms regulating regional localization of inflammation during CNS autoimmunity. Immunol Rev 2012;248:205–15.
8. Vos CMP, Geurts JJG, Montagne L, van Haastert ES, Bo L, van der Valk P, et al. Blood-brain barrier alterations in both focal and diffuse abnormalities on postmortem MRI in multiple sclerosis. Neurobiol Dis 2005; 20:953–60.
9. Janssen BJC, Robinson RA, Perez-Branguli F, Bell CH, Mitchell K, Siebold C, et al. Structural basis of semaphoring-plexin signaling. Nature 2010;467: 1118–22.
10. Elhabazi A, Delaire S, Bensussan A, Boumsell L, Bismuth G. Biological activity of soluble CD100: the extracellular region of CD100 is released from the surface of T lymphocytes by regulated proteolysis. J Immunol 2001;166:4341–7.
11. Delaire S, Elhabazi A, Bensussan A, Boumsell L. CD100 is a leukocyte semaphorin. Cell Mol Life Sci 1998;54:1265–76.
12. Kumanogoh A, Watanabe C, Ihnsook L, Wang X, Shi W, Hiraki H, et al. Identification of CD72 as a lymphocyte receptor for the class IV semaphorin CD100: a novel mechanism for regulating B cell signaling. Immunity 2000;13:621–31.
13. Kumanogoh A, Kazuhiro S, Ch'ng E, Watanabe C, Marukawa S, Takegahara N, et al. Requirement for the lymphocyte semaphorin, CD100, in the induction of antigen-specific T cells and the maturation of dendritic cells. J Immunol 2002;169:1175–81.
14. Moreau-Fauvarque C, Kumanogoh A, Camand E, Jaillard C, Barbin G, Boquet I, et al. The transmembrane semaphorin sema4D/CD100, an inhibitor of axonal growth, is expressed on oligodendrocytes and upregulated after CNS lesion. J Neurosci 2003;23:9229–39.
15. Smith E, Jonason A, Reilly C, Veeraraghavan J, Fisher T, Doherty M, et al. SEMA4D compromises blood-brain barrier, activates microglia and inhibits remyelination in neurodegenerative disease. Neurobiol Dis 2015;73: 254–68.

16. Zhu L, Bergmeier W, Wu J, Jiang H, Stalker TJ, Cieslak M, et al. Regulated surface expression and shedding support a dual role for semaphorin 4D in platelet responses to vascular injury. Proc Natl Acad Sci U S A 2007; 104:1621–6.
17. Tamagnone L, Artigiani S, Chen H, He Z, Ming GI, Song H, et al. Plexins are a large family of receptors for transmembrane, secreted, and GPI-anchored semaphorins in vertebrates. Cell 1999;99:71–80.
18. Giordano S, Corso S, Conrotto P, Artigiani S, Gilestro G, Barberis D, et al. The semaphorin 4D receptor controls invasive growth by coupling with Met. Nat Cell Biol 2002;4:720–4.
19. Giraudon P, Vincent P, Vuaillat C, Verlaeten O, Cartier L, Marie-Cardine A, et al. Semaphorin CD100 from activated T lymphocytes induces process extension collapse in oligodendrocytes and death of immature neural cells. J Immunol 2004;172:1246–55.
20. Giraudon P, Vincent P, Vuaillat C. T-cells in neuronal injury and repair: semaphorins and related T-cell signals. Neuro Mol Med 2005;7:207–16.
21. Basile J, Gavard J, Gutkind JS. Plexin-B1 utilizes RhoA and RhoK kinase to promote the integrin-dependent-activation of Akt and ERK and endothelial cell motility. J Biol Chem 2007;282:34888–95.
22. Liang X, Draghi N, Resh M. Signaling from integrins to fyn to rho family GTPases regulates morphologic differentiation of oligodendrocytes. J Neurosci 2004;24:7140–9.
23. Niederost B, Oertle T, Fritsche J, McKinney RA, Bandtlow C. Nogo-A and myelin-associated glycoprotein mediate neurite growth inhibition by antagonistic regulation of rhoA and rac1. J Neurosci 2002;22:10368–76.
24. Witherden DA, Watanabe M, Garijo O, Rieder SE, Sarkisyan G, Cronin SJF, et al. The CD100 receptor interacts with its plexin B2 ligand to regulate epidermal $\gamma\delta$ T cell function. Immunity 2012;37:314–25.
25. Kumanogoh A, Kikutani H. The CD100-CD72 interaction: a novel mechanism of immune regulation. Trends Immunol 2001;22:670–6.
26. Basile JR, Castillo RM, Williams VP, Gutkind JS. Semaphorin 4D provides a link between axon guidance processes and tumor-induced angiogenesis. Proc Natl Acad Sci U S A 2006;103:9017–22.
27. Sierra JR, Corso S, Caione L, Cepero V, Conrotto P, Cignetti A, et al. Tumor angiogenesis and progression are enhanced by Sema4D produced by tumor-associated macrophages. J Exp Med 2008;205:1673–85.
28. Bismuth G, Boumsell L. Controlling the immune system through semaphorins. Sci STKE 2002;2002(128):re4.
29. Valente G, Nicotra G, Arrondini M, Castino R, Capparuccia MP, Kerim S, et al. Co-expression of plexin-B1 and Met in human breast and ovary tumours enhances the risk of progression. Cell Oncol 2009;31: 423–36.
30. Delaire S, Billard C, Tordjman R, Chédotal A, Elhabazi A, Bensussan A, et al. Biological activity of soluble CD100: Soluble CD100, similarly to H-SemaIII, inhibits immune cell migration. J Immunol 2001;166:4348–54.
31. Hall KT, Boumsell L, Schultze JL, Boussiotis VA, Dorfman DM, Cardoso AA, et al. Human CD100, a novel leukocyte semaphorin that promotes B-cell aggregation and differentiation. Proc Natl Acad Sci U S A 1996;93: 11780–5.
32. Southwell A, Franciosi S, Villanueva EB, Xie Y, Winter LA, Veeraraghavan J, et. al. Anti-semaphorin 4D immunotherapy ameliorates neuropathology and some cognitive impairment in the YAC128 mouse model of Huntington disease. Neurobiol. Epub 2015 Feb 3.
33. Evans E, Jonason A, Bussler H, Torno S, Veeraraghavan J, Reilly C, et al. Antibody blockade of Semaphorin 4D promotes tumor rejection and improves response to immunomodulatory therapies. Cancer Immunol Res. Epub 2015 Jan 22.
34. Labrijn AF, Buijsse AO, van den Bremer ET, Verwilligen AY, Bleeker WK, Thorpe SJ, et al. Therapeutic IgG4 antibodies engage in Fab-arm exchange with endogenous human IgG4 *in vivo*. Nat Biotechnol 2009;27:767–71.
35. Fisher TL, Pandina T, Winter LA, Reilly C, Jonason A, Scrivens M, et al. Discovery and characterization of an antibody specific for SEMA4D: implications for treatment in oncology, autoimmune and neurodegenerative disease. 2015; forthcoming.
36. Heider KH, Kiefer K, Zenz T, Volden M, Stilgenbauer S, Ostermann E, et al. A novel Fc-engineered monoclonal antibody to CD37 with enhanced ADCC and high proapoptotic activity for treatment of B-cell malignancies. Blood 2011;118:4159–68.
37. Burleson GR, Burleson FG. Testing human biological in animal host resistance models. J Immunotoxicol 2008;5:23–31.
38. Burleson GR, Burleson FG. Influenza virus host resistance model. Methods 2007;41:31–7.
39. Bourdage J, Cook C, Farrington DL, Chain JS, Konrad RJ. An affinity capture elution (ACE) assay for detection of anti-drug antibody to monoclonal antibody therapeutics in the presence of high levels of drug. J Immunol Methods 2007;327:10–7.
40. Chamanza R, Marksfield HA, Blanco AI, Naylor SW, Bradley AE. Incidences and range of spontaneous findings in control cynomolgus monkeys (Macaca fascicularis) used in toxicity studies. Toxicol Pathol 2010;38: 642–57.
41. Wang W, Wang EQ, Balthasar JP. Monoclonal antibody pharmacokinetics and pharmacodyamics. Nature 2008;84:548–58.
42. Martin P, Jiao Q, Cornacoff J, Hall W, Saville B, Nemeth JA, et al. Absence of adverse effects in cynomolgus macaques treated with CNTO 95, a fully human anti-αv integrin monoclonal antibody, despite widespread tissue binding. Clin Cancer Res 2005;11:6959–65.
43. Labrijn AF, Aalberse RC, Schuurman J. When binding is enough: non-activating antibody formats. Curr Opin Immunol 2008;20:479–85.
44. Wierda D, Smith H, Zwickl CM. Immunogenicity of biopharmaceuticals in laboratory animals. Toxicology 2001;158:71–4.
45. Beers SA, French RR, Chan HTC, Lim SH, Jarrett TC, Vidal RM, et al. Antigenic modulation limits the efficacy of anti-CD20 antibodies: implications for antibody selection. Blood 2010;24:5191–201.
46. Gordon MS, Margolin K, Talpaz M, Sledge GW Jr, Holmgren E, Stalter S, et al. Phase I safety and pharmacokinetic study of recombinant human anti-vascular endothelial growth factor in patients with advanced cancer. J Clin Oncol 2001;19:843–50.

Published OnlineFirst February 5, 2015; DOI: 10.1158/1535-7163.MCT-14-0924

Molecular Cancer Therapeutics

Nonclinical Safety Evaluation of VX15/2503, a Humanized IgG4 Anti-SEMA4D Antibody

John E. Leonard, Terrence L. Fisher, Laurie A. Winter, et al.

Mol Cancer Ther 2015;14:964-972. Published OnlineFirst February 5, 2015.